FERMILAB PROPOSAL NO. 446

Correspondent: C. Ankenbrandt
Fermilab, X4005

The Direct Determination of Kaon and Pion Form Factors

C. Ankenbrandt, R. Brown,* S. Ecklund, P. J. Gollon,
J. Lach, J. MacLachlan, A. Roberts, G. Shen
Fermi National Accelerator Laboratory

L. A. Fajardo, R. Majka, J. N. Marx, P. Nemethy,
J. Sandweiss, A. Schiz, A. J. Slaughter
Yale University

October 1975

*Visitor from Rutherford Laboratory, Chilton, Didcot,
Berkshire, England.

I. INTRODUCTION

We propose an experiment to determine the kaon and pion electromagnetic form factors directly and precisely. Since the earliest formal studies of the experimental program at the laboratory now known as Fermilab, it has been recognized that the availability of high energy beams of mesons would provide an exciting new opportunity to probe their electromagnetic structure.[1-5] The form factors $F_M(Q^2)$ ($M = \pi$ or K) characterizing this structure can be determined directly by comparing the observed cross sections $\frac{d\sigma}{dQ^2}$ for elastic scattering from atomic electrons to the hypothetical values in the absence of structure:

$$|F_M(Q^2)|^2 = \left(\frac{d\sigma}{dQ^2}\right) \Big/ \left(\frac{d\sigma}{dQ^2}\right)_{\text{pointlike}} .$$

The form factor can be regarded as the Fourier transform of the meson's spatial charge distribution. The low-Q^2 behavior of $F(Q^2)$ then determines the mean-square charge radius:

$$F(Q^2) = 1 - R_M^{\,2}\, Q^2/6 + \ldots ,$$

where $R_M \equiv \sqrt{< r_M^{\,2} >}$. If a one-pole parameterization is adopted, then the pole mass is inversely proportional to the charge radius:

$$F(Q^2) = \frac{1}{1 + Q^2/M_{\text{eff}}^{\,2}} \approx 1 - Q^2/M_{\text{eff}}^{\,2},$$

so that $R_M = \sqrt{6}\,\hbar c/M_{eff}$. We expect to determine the kaon charge radius to about 6% and the pion radius simultaneously to about 2-3%.

II. PRESENT KNOWLEDGE

Although the nature of both theoretical approaches and experimental methods should be similar in principle for the pion and kaon form factors, work to date has in fact heavily emphasized the pion case, as the following review suggests.

A. Theoretical Expectations

Theoretical insight into the expected behavior of the meson form factors has come from two complementary approaches, one general and one specific. First, the set of assumptions characterized loosely by the phrase "microscopic causality" leads to dispersion relations connecting the spacelike region of direct interest in this proposal with the time-like region explored in electron-positron colliding beam experiments ($e^+e^- \rightarrow \pi^+\pi^-$, K^+K^-). When the existing data on meson production in electron-positron colliding beam experiments in the time-like region are inserted into these relations, together with "reasonable" extrapolations into unmeasured regions, there result bounds on the allowed variation of the spacelike form factor. Such bounds are slightly dependent on the details of the assumptions that enter the calculation; typical limits have been derived by Levin and Okubo[6]: $0.28 \leq R_\pi^2 \leq 0.47\ \mathrm{fm}^2$. A recent preprint by Kiehlmann and

Schmidt[7] has re-examined the analyticity question in the light of new data; they deduce the following fairly precise result for the mean-square pion radius: $R_\pi^2 = (0.46 \begin{smallmatrix} +0.06 \\ -0.08 \end{smallmatrix})\ \mathrm{fm}^2$. The accuracy and precision of such results will continue to improve as colliding beam data over a wider energy range are incorporated in the calculations. Similar results for F_K should be derivable from the kaon pair production data; however the threshold of the timelike experiments, $|Q^2| = 4m_K^2$, is much further from the spacelike region than in the pion case, complicating the calculation.

Specific models can also be invoked to predict the behavior of the meson form factors. To take the best-known example, the vector dominance model (VDM)[8] predicts that the pion form factor is dominated by the ρ meson pole:

$$F_\pi^{VDM}(Q^2) = \frac{1}{1 + Q^2/m_\rho^2} .$$

A similar result for F_K is expected to involve ρ, ω, and ϕ mesons; the SU_3 prediction[16] for the relative contributions is

$$F_K^{VDM}(Q^2) = \frac{1}{2}\left(\frac{1}{1 + Q^2/m_\rho^2}\right) + \frac{1}{8}\left(\frac{1}{1 + Q^2/m_\omega^2}\right) + \frac{3}{8}\left(\frac{1}{1 + Q^2/m_\phi^2}\right).$$

These vector dominance predictions imply that $R_\pi = 0.63$ fermi ($R_\pi^2 = 0.4\ \mathrm{fm}^2$) and $R_K = 0.58$ fermi ($R_K^2 = 0.34\ \mathrm{fm}^2$).

Several authors[8-10] have examined possible relationships between F_π and various components of the nucleon form factors.

Some of these ideas lead to values of the pion radius larger than the ρ dominance prediction. Long ago Drell[5] emphasized the theoretical interest in determining the difference if any between the pion and nucleon radii. A difference in size is suggested by the naive uncertainty principle argument that a nucleon can emit a single virtual pion but a pion cannot because of G parity.

B. Experimental Situation

1) Direct Measurements

The direct determination of meson form factors by meson-electron scattering benefits greatly from the highest feasible beam energy because the maximum momentum transfer Q^2_{max} kinematically possible in meson-electron scattering is severely limited by the light mass of the electron target, but rises rapidly with energy. To review some familiar kinematics, recall that

$$Q^2 \equiv -t = 2\, P^{*2}\, (1 - \cos\theta^*)$$

$$\therefore\ Q^2_{max} = 4\, P^{*2} = \frac{4\, p^2_{beam}\, m_e^{\,2}}{s}$$

where $s = M^2 + 2\, m_e\, E_{beam} + m_e^{\,2}$ and $M = m_\pi$ or m_K. These quantities are evaluated at 200 GeV/c, the highest energy we propose to use, in Table I. Note that at this energy, vector dominance predicts that the cross section at Q^2_{max} is 58% of the pointlike cross section for pions and 78% for kaons.

TABLE 1

MESON-ELECTRON SCATTERING CHARACTERISTICS AT 200 GeV/c

Beam Particle	$s\,(\mathrm{GeV}^2)$	$Q^2_{max}\,(\mathrm{GeV/c})^2$	$\left(\frac{d\sigma}{dQ^2}\right)^{VDM} \Big/ \left(\frac{d\sigma}{dQ^2}\right)_{pt}$ at Q^2_{max}
π	0.2239	0.1866	0.58
K	0.4481	0.0932	0.78

Published attempts to exploit the direct method have suffered from limited available beam energy. For example, the beam energy at which vector dominance predicts a significant deviation of the form factor from unity, say $|F^{VDM}(Q^2_{max})|^2$ is 0.8, is 84 GeV/c for pions and 189 GeV/c for kaons. Crawford[11] used a 1.12 GeV/c π^- beam producing δ-rays in a hydrogen bubble chamber and found results consistent with the pointlike cross section as expected. Subsequent experiments[12-13] used 16 and 20 GeV/c pion beams and obtained rather non-restrictive limits on the pion radius as summarized in Table 2.

TABLE 2

SUMMARY OF DIRECT PION FORM FACTOR EXPERIMENTS

Reference	P_{beam} (GeV/c)	Detector	Result	
11	1.12	H_2 bubble chamber	Consistent with point-like	
12	16	H_2 bubble chamber	$R_\pi < 4.5$ fm	
13	20	Spark chambers	$R_\pi < 3$ fm	
14	50	Spark chambers	$R_\pi = 0.95 \pm 0.12$ fm	same expt.
16	"	"	$R_\pi = 0.96 \pm 0.06$ fm	same expt.
15	"	"	$R_\pi = 0.78 \pm 0.10$ fm	same expt.
16 - 18	100	Spark chambers and PWC's	Just finished running	

The highest-energy results reported[14-16] to date come from a JINR-UCLA experiment in a 50 GeV/c pion beam at Serpukhov. These experimenters originally reported results differing significantly from the vector dominance prediction and even violating the analyticity bound, but later reports converged toward the theoretical expectations as shown in Table 2. Nevertheless the experiment is the most interesting published attempt to determine the pion form factor directly. A similar experiment, UCLA-Notre Dame-Pittsburgh-Fermilab-JINR experiment E-216,[16] has just completed data-taking in a 100 GeV/c π^- beam at Fermilab; some technical results from this latter experiment are available in the form of a Progress Report submitted to the laboratory in May 1975.[17]

The aforementioned direct experiments have all concerned pions. To our knowledge, no data exist on the direct determination of kaon form factors. (The E-216 proposal expressed the hope of accumulating kaon data but the experiment did not in fact do so.)

2) Indirect Determinations

Indirect methods have also been applied to learn something about the pion form factor. The electroproduction of pions is an example wherein the form factor contribution in a diagram such as that of Fig. 1(b) is isolated.[19] This approach has the advantage that energetic virtual photons are involved and considerably larger ranges of Q^2 are thus probed than in the direct experiments. However the method is unavoidably model-dependent and could also be regarded as a test of the ability of the experimenters to isolate the contribution of a particular Feynman diagram and of the theorists to calculate it correctly.

Attempts to apply the electroproduction method to the kaon form factor are complicated by difficulties in separating the K^* exchange diagram (Fig. 1(d)) from the desired K exchange diagram (Fig. 1(c)).[20] Although the electroproduction of kaons has been observed,[21] no form factor result was quoted.

Experiments have also used the scattering of pions from helium nuclei,[22] but the results are rather imprecise.

In reviewing our present knowledge, the lack of experimental information on the kaon form factor stands out most strikingly. We believe that the apparatus to be described in the next section is the ideal tool with which to explore this virgin territory.

III. EXPERIMENTAL DESIGN

A. Introduction

The configuration of the apparatus is shown in Fig. 2(a). This arrangement is a minor modification of the existing apparatus of E69 (Fig. 2(b)), which has been described previously.[23] For completeness we present here a self-contained discussion of the equipment.

As we shall see, the outstanding features of the system are high spatial resolution and great data rate capability. The spatial resolution, due primarily to the use of high-pressure PWC's with small wire spacing, leads to excellent angular and momentum resolution. The data rate capability results from the following factors:

1) All position-measuring detectors are PWC's whose time resolution allows beam fluxes in excess of 10^6/sec;
2) Sophisticated triggering rejects events with uninteresting PWC hit topologies before they are read into our PDP-15 computer;
3) The computer is able to record up to 800 interesting events per spill.

These capabilities of the system, angular resolution and data rate, are precisely the key factors in the success of the π-e and K-e experiments, as will become apparent in the ensuing discussions.

The experience of the Serpukhov and E216 experiments, since it is the highest energy information available, is probably the

easiest to extrapolate to our energies. For this reason and also because the E216 collaboration has recently expressed its intention[18] to submit a new proposal for their apparatus covering kaons as well as pions at higher energies than their recent experiment, we will occasionally compare the capabilities of our apparatus with these other experiments. A large advantage of our apparatus over that of E-216 is in the beam flux capability of 10^6/sec; E-216 ran with about 10^5/sec. This is particularly important for the kaon form factor determination.

B. Apparatus

1) Beam

The incident beam, the west branch of the M6 line in the Meson Lab, is a 3-stage beam. A PWC at the 2nd (momentum-dispersed) focus tags the momentum of individual beam particles to within 0.03%. (The parameters of all the PWC's are summarized in Table 3.)

The beam particles are reliably identified by a series of Cerenkov counters. There is a differential counter of SLAC design used to identify protons and antiprotons, a CERN DISC for $K^{\pm}$, and a set of threshold counters for $\pi^{\pm}$.

2) Target Area

The beam impinges on a 52.4 cm long liquid hydrogen target of conventional Fermilab design. The target is surrounded by lead and scintillation counters to discriminate strongly against events with extra charged or neutral particles in the final state. For the events of interest, both particles emerge through a small hole in the forward direction.

3) Angular Measurements

The importance of angular resolution arises from the same effect that biases us in favor of the highest feasible beam energies, namely the severe limitation on Q^2. Small Q^2 means small transverse momentum, which in turn implies very small lab angles in the final state (cf. Fig. 3). Thus a small-angle, high resolution forward spectrometer is ideally suited, nay essential, for the experiment.

The importance of angular resolution is exemplified by the Serpukhov experiment.[15] Difficulties in reliably sorting out two-track events apparently caused the largest systematic errors in that experiment, wherein two independent programs led to values of $R_\pi^2 = 0.47\ fm^2$ and $R_\pi^2 = 0.72\ fm^2$.

The E216 experimenters have recently undertaken the addition of drift chambers downstream of their target to improve the angular resolution for their desired higher energy running. Our experiment uses closely spaced PWC wires to achieve resolution with much lower intensities per wire.

The angles of incoming and outgoing trajectories are measured by means of four clusters of high-resolution PWC's labeled A, B, C, D in Fig. 2(a), two on either side of the target. These detectors rest on a long reinforced concrete block in a temperature-controlled environment for stability. Measured spatial resolutions of ±60-70 microns in each cluster together with lever arms of 3-4 meters result in angular resolutions of about ± 30 micro-radians on incoming and outgoing tracks. The align-

ment and resolution are continuously monitored by triggering on a prescaled fraction of beam tracks.

TABLE 3

CHARACTERISTICS OF PROPORTIONAL WIRE CHAMBERS

Name	Coordinate(s) measured	Effective wire spacing	Aperture	Gas
P	X	1 mm	R = 4.8 cm	1 atm Ar-CO_2
A	XY	0.2 mm	R = 1.5 cm	3.4 atm magic gas
B	XY	0.2 mm	R = 1.5 cm	3.4 atm magic gas
C	XYUV	0.2 mm	R = 1.5 cm	3.4 atm magic gas
D	XY	0.2 mm	R = 3.0 cm	3.4 atm magic gas
E	UV	1.5 mm	R = 4.8 cm	1 atm Ar-CO_2
F	XY	1.5 mm	R = 4.8 cm	1 atm Ar-CO_2
G	X	1 mm	15 x 30 cm	1 atm Ar-CO_2
H	Y	10 mm	15 x 30 cm	1 atm Ar-CO_2

The D cluster is preceded by a conventional PWC cluster labeled E of larger aperture whose purpose is to extend the Q^2 range down to $Q^2 \approx 0.014$ by detecting the larger-angle (up to 10 mr) electron recoils associated with low Q^2 events.

4) Momentum Spectrometer

The final-state momentum measurement is important not just as an added constraint on the elastic scattering hypothesis but because

it is directly related to Q^2. In fact Q^2 is proportional to the recoil electron kinetic energy T_e,

$$Q^2 = 2\ m_e\ T_e.$$

By conservation of energy then Q^2 is also proportional to the energy loss of the meson,

$$Q^2 = 2\ m_e\ (E_{beam} - E_{M,\ final}),$$

and one can measure Q^2 directly by measuring the momentum of either final state particle. There is some advantage to measuring the final-state meson in that it is not subject to radiative losses in emerging from the target, and this is what we plan to do in almost all cases.

In our spectrometer, a main-ring dipole magnet just downstream of the fourth high resolution chamber disperses the scattered particles. A conventional PWC labeled G in Fig. 2(a), about 40 feet downstream of this magnet, together with the angular information from Clusters C and D upstream, determines the bend angles and hence the momentum. The PWC's labeled F and H provide additional coordinate measurements for redundancy.

The momentum acceptance of the spectrometer covers the range $\frac{1}{2}\ p_{beam} \leq p \leq p_{beam}$. For K-e scattering the kaon momentum lies within this interval for all Q^2. For π-e scattering at 200 GeV/c the pion momentum will be measured for $Q^2 \lesssim 0.1$ (p_π =

= 100 GeV/c); furthermore when we run negative beam we will measure the electron momentum in the rest of the range: $0.1 < Q^2 < Q^2_{max}$. Thus with a modest-sized spectrometer we can cover the entire Q^2 region of interest for $K^{\pm}$ and π^- with a single setting at each polarity, and more than half the Q^2 range for π^+.

The angular acceptance is sufficient to detect <u>all</u> K-e events above about $Q^2 \approx 0.014$; for the π-e scatters there is a slight reduction in azimuthal acceptance near $Q^2 \approx \frac{1}{2} Q^2_{max}$ (cf. Fig. 4).

The resolution on the momentum measurement is expected to be 0.22% at 200 GeV/c, including both chamber resolution and multiple scattering.

The final elements of the spectrometer are a lead-scintillator sandwich shower counter to identify electrons followed by an iron-scintillator sandwich hadron calorimeter to discriminate against muons.

C. Event Reconstruction

We have a "3C" fit to the electron scattering hypothesis throughout the detected Q^2 range. Both outgoing angles are accurately measured as well as the momentum of the more energetic secondary.

Giving up the momentum measurement on the lower-momentum secondary has several advantages:

1) It allows us to cover the Q^2 range down to $Q^2 \approx 0.014$ in a single setting with a one-arm momentum spectrometer of reasonable size.

2) It enables us to do both beam polarities with the said spectrometer. E216 and the Serpukhov experiment used only π^-.

Results from the Serpukhov experiment show that the constraint that we are relaxing, that $p_e + p_M = p_{beam}$, is the least effective of the four kinematical constraints in reducing hadronic background.[16] We feel that our good resolution on the other three constraints will be more than adequate to eliminate hadronic backgrounds that escape the target veto system.

D. Required Modifications to Apparatus of E69

That the modifications to the present apparatus of E69 are relatively minor can be seen by comparing Fig. 2(a) and (b). The changes are necessary to increase both the angular acceptance and the momentum acceptance of the spectrometer.

The momentum acceptance is increased from about 19% to more than 50% by removing one magnet and shortening the downstream lever arm. The resulting momentum resolution of about 0.22% is still quite sufficient for the experiment. The lever arm is reduced by removing two of the three 30-foot sections of the Cerenkov counter. (The name "Cerenkov counter" is kept for historical reasons; with this length at these energies, it is best regarded as a vacuum pipe with rather poor vacuum.)

The angular acceptance is increased by removing the downstream magnet, thereby moving the limiting aperture upstream, by enlarging the active area of PWC cluster D and by providing cluster E as an "electron catcher". We will also need to provide additional channels of readout electronics for the new PWC wires.

This section has tried to establish that the existing apparatus of Experiment 69, with minor modifications, is ideally suited to perform these measurements. In fact, a prominent signal due to scattering from electrons at low Q^2 stands out in the event sample of E69. Figure 5 illustrates the clean separation of π-e scatters from hadronic background in a typical E69 run, using only the forward spectrometer with no measurement of the angle of the electron.

IV. CROSS SECTIONS AND RATES

A. Pointlike Cross Section

The "pointlike cross section" describing the scattering of hypothetical structureless spin-zero particles by electrons is given to lowest order in the fine-structure constant by the expression

$$\left(\frac{d\sigma}{dQ^2}\right)_{\text{pointlike}} = \frac{4\pi\ \alpha^2}{(Q^2)^2} \left\{\frac{1}{\beta^2} - \frac{Q^2}{Q_{max}^2}\right\},$$

where $Q^2 \equiv -t$, the invariant four momentum transfer squared, is positive in the physical (spacelike) region, and β is the lab velocity of the incident meson. This expression can be integrated from a positive lower limit Q_{low}^2 to the kinematic limit. Taking $Q_{low}^2 \cong 0.014$ as appropriate for this proposal, we find pointlike cross sections at 200 GeV/c of about 14 μb for pions and 11 μb for kaons. The cross sections integrated over various representative Q^2 ranges at 200 GeV/c are tabulated below.

TABLE 4

POINTLIKE CROSS SECTIONS INTEGRATED FROM Q^2_{low} TO KINEMATIC LIMIT

	Q^2_{low} $(GeV/c)^2$	Cross Section (μb)
π-e	0.014	13.6
	0.05	1.98
(Q^2_{max} = 0.1866)	0.09	0.48
	0.13	0.10
K-e	0.013	11.7
(Q^2_{max} = 0.932	0.05	0.67

B. Error Matrix Estimations

The question of how many events are needed for a form factor determination of specified accuracy is complicated. The events cluster at low Q^2, but the high Q^2 events are the most sensitive to deviations of the form factor from unity. Furthermore, the form factor determination is obviously sensitive to errors in absolute normalization, but the normalization can be checked by measuring to low enough Q^2 so that $F(Q^2_{low}) \approx 1$.

To quantify these considerations, we have calculated the error matrix that would apply after N_{beam} particles if the measured cross section is fit by

$$\frac{d\sigma}{dQ^2} = A_{norm} \left(\frac{d\sigma}{dQ^2}\right)_{ptlike} \left|F(Q^2)\right|^2,$$

where $F(Q^2) = (1 + Q^2/m_{eff}^2)^{-1}$ and A_{norm} is a normalization constant with an expected value of unity and an a priori uncertainty of σ_A. We obtain then a two-by-two error matrix involving the uncertainties in A_{norm} and in m_{eff}. The fractional error in m_{eff} is shown in Fig. 6 as a function of running time at 200 GeV/c for various assumed values of normalization uncertainty σ_A, using the Q_{low}^2 applicable to our experiment and assuming m_{eff} is close to the vector dominance prediction.

As a working hypothesis we estimate that the experiment may be subject to systematic errors around the 5-10% level in $(\Delta m_{eff}/m_{eff})$ or equivalently in $(\Delta r/r)$ for kaons. We aim then for comparable statistical errors for the kaon data. The statistical uncertainty on the simultaneously accumulated pion data will then be very small. In fact we will have sufficient pion statistics to study the systematic errors empirically; this will lead to a better kaon experiment. As a simple example, the normalization of the pion data will be determined very well by the extrapolation to $Q^2 = 0$; this same normalization can be used for the kaon data.

Table 5 below outlines a set of runs that achieves these statistical goals, assuming a priori normalization uncertainty of 3%.

TABLE 5

SUMMARY OF STATISTICS EXPECTED

P_{beam}	Running Time	Beam Particle	Total No. Inc. Beam	No. of Events	$\frac{\Delta m}{m} = \frac{\Delta r}{r}$	Q^2 range
+200	200 hrs	K	1.35×10^9	3.2×10^4	8.1%	0.013-0.093
		π	4.5×10^9	9.8×10^4	2.9%	0.014-0.1
-200	200	K	1.35×10^9	3.2×10^4	8.1%	0.013-0.093
		π	9×10^9	2.4×10^5	1.7%	0.014-0.186
-150	200	K	1.35×10^9	2.8×10^4	12.3%	0.012-0.058
		π	9×10^9	2.2×10^5	2.2%	0.014-0.136

Many assumptions enter in translating from number of events desired to running time needed; we have used the following numbers in calculating Table 5:

Target length = 52.4 cm → 2.19 events per barn per incident particle.

Duty cycle: 1 sec spill at 8 sec. intervals.

Beam flux: 10^6 particles/second (attainable even at -200 GeV/c with 2×10^{12} 400 GeV/c protons on the meson lab target.)

Beam composition: The (detected K/all charged) ratio is

observed to be close to 3% for both energies, both polarities in M6W. We assume then 30,000 $K^{\pm}$/spill. To avoid saturating our data acquisition system we will prescale the predominant particles as in E69 to limit the sampled beam to about 2×10^5/spill. For positives this will be split between pions and protons. Thus we assume

$$N_{\pi+} = 10^5/\text{spill}$$

$$N_{\pi-} = 2 \times 10^5/\text{spill}$$

Safety factor: There is a safety factor of two in translating from incident flux to running time in Table 5.

C. Trigger Requirements and Rates

The event selection logic will be very similar to that of E69. The two-level system consists of a conventional scintillator pretrigger implemented in commercial fast logic, followed by fast analog circuitry which selects events with interesting PWC topologies for input to our PDP-15 computer.

The scintillator pretrigger enforces the following requirements:

(a) A beam particle is unaccompanied by others within ±100 nsec ($B1 \cdot B2 \cdot \overline{VH1}$ in Fig. 1);

(b) Beam veto V1 at the third focus is not struck;

(c) S1 indicates a particle traversing the momentum spectrometer;

(d) The vetos around the target are quiet.

Requirements (a) - (c) are in the E69 pretrigger; the target counters of (d) were merely latched in E69 to allow us to accumulate inelastic events in an unbiased way.

The analog arithmetic units demand the following criteria of an event candidate:

(a) The "HFD" (hardware focus detector) requires that the beam particle trajectory upstream of the target is in the beam phase space, headed for the beam veto, in both views;

(b) The "HSD" (hardware scatter detector) requires that clusters A, B, and D show a kink in the target vicinity;

(c) The "HMD" (hardware momentum determiner) requires that clusters C, D, and G indicate an outgoing momentum significantly different from p_{beam}.

The HFD and HSD have thoroughly established their reliability, stability and utility in E69. The HMD, which is new, will be very similar in design to the existing devices.

The similarity in trigger to that of E69 means that we can reliably extrapolate our past experience to calculate trigger rates, adopting conservative estimates for the rate reductions from the HMD and the target vetoes. This extrapolation predicts that with the running conditions outlined in the preceding section we will examine 2×10^4 pretriggers per spill and accept 300 triggers, of which about 2/3 will be hadronic elastic scatters and 1/3 will be inelastics. The event rate for the reaction of

interest will be a few per spill. These rates are comfortably within our capabilities and will result in about 25% deadtime during a one-second spill. If necessary we can easily achieve a further large trigger rate reduction by implementing a forward multiplicity ≥ 2 requirement, but we would prefer to impose this condition off-line, keeping the trigger free of this sort of possible bias.

IV. CONTROL OF SYSTEMATIC ERRORS

The control of systematic errors is obviously of paramount importance in this experiment. We have already described some of the ways in which our experimental design will serve to minimize such errors. This section outlines further aspects of our planning in this regard.

A. Normalization

The need for careful normalization is apparent since we want to determine the ratio of the observed cross section to the pointlike cross section. We have two independent checks of our normalization:

1) As in our elastic hadron-proton scattering experiment E69, the incident beam will pass through all our detectors, and a prescaled fraction of the beam will be accepted in the trigger. To require that the beam particles accepted for normalization purposes be detected by all the same detectors required for the events of

interest is an accurate normalization technique whose value was proved in E69. Essentially the same technique will be applicable here.

2) Secondly we will measure (in the same setup and at the same time as the main data-taking run) the form factor at a Q^2 small enough so that the extrapolation to $Q^2 = 0$, where the form factor is required to be unity, provides a tight constraint on the normalization. Our design is fully sensitive down to Q^2 of 0.014, at which point vector dominance predicts $F_\pi = 0.977$ and $F_K = 0.980$.

B. Consistency Checks

We will simultaneously accumulate π, K, and (p or $\bar{p}$) events, which serves to cross-check the results. Besides the K-π cross-checking, the proton form factors are well known and thus p-e scattering is a useful calibration reaction.

We will accumulate data for both beam polarities. The form factor results must be the same; however the contributions of some of the diagrams describing radiative corrections change sign with the beam charge. We can thereby check our radiative correction calculations.

We also plan to accumulate data at two energies. The requirement that the form factors depend only on Q^2 and not on p_{beam} is a further consistency check.

VI. REQUESTS

We will have the new elements of the apparatus ready to install when our hadronic measurements (including the complex nuclear target data) are complete, say by July 4, 1976. The reconfiguration for this experiment would then take a few weeks, preferably while the East branch of the beam line is used. A week of testing with beam would be required next to check out the new detectors and electronics. We would then be ready to proceed with the measurement matrix outlined above: -200 GeV/c, +200 GeV/c, and -150 GeV/c with about 200 beam hours at each setting. Allowing for testing, tuning and contingencies, we request 800 hours of beam time. We also ask for 100 hours of 6600 CPU time for rapid turnaround computing as well as continued use of PREP equipment presently allotted to E69.

VII. SUMMARY

We propose to determine the electromagnetic form factor of the kaon and that of the pion directly by comparing their observed elastic scattering from atomic electrons with the cross section expected in the absence of structure. The experiment takes advantage of the excellent rate and resolution characteristics of the existing E69 apparatus, suitably modified to increase its acceptance.

Analyticity relates this spacelike form factor with the timelike domain explored in colliding beam experiments ($e^+e^- \to K^+K^-$, $\pi^+\pi^-$). Vector dominance predicts the following forms:

$$F_\pi(Q^2) = (1 + Q^2/m_p{}^2)^{-1}$$

$$F_K(Q^2) = \frac{1}{2}(1 + Q^2/m_p{}^2)^{-1} + \frac{1}{8}(1 + Q^2/m_\omega{}^2)^{-1} + \frac{3}{8}(1 + Q^2/m_\phi{}^2)^{-1}$$

The vector dominance predictions imply that the charge radii, defined by $R^2 = -6 \left.\frac{dF}{dQ^2}\right|_{Q^2 = 0}$, are $R_\pi = 0.63$ fermi and $R_K = 0.58$ fermi.

Previous direct experiments have not determined the pion form factor very precisely, and there is no experimental information, direct or indirect, on the kaon form factor in the spacelike region.

We request 800 hours of beam time equally divided among -200 GeV/c, +200 GeV/c, and -150 GeV/c. We will accumulate about 9×10^4 K-e events and 5.6×10^5 π-e events, leading to a 6% determination of R_K and a simultaneous 2-3% determination of R_π.

REFERENCES

[1]T. Toohig, "An Experiment to Measure the Pion Form Factor at the 200 GeV Accelerator", Vol. 1, p. 144 of 200 BeV Accelerator: Studies on Experimental Use, UCRL-16830, 1966.

[2]J. A. Poirier, "The Electromagnetic Form Factor of the Charged Pion (Muon, Kaon, Electron)", Vol. 3, p. 49 of 1968 NAL Summer Study.

[3]Richard Wilson, "Comments on 'The Electromagnetic Form Factor of the Charged Pion' by J. A. Poirier", ibid. p. 57.

[4]D. Luckey, "Form Factor Experiments", ibid. p. 59.

[5]S. D. Drell, "Remarks on Experiments at NAL", ibid. p. 327.

[6]David N. Levin and Susumu Okubo, "Can the Pion's Charge Radius be Large?", Phys. Rev. D6, 3149 (1972).

[7]H.-D. Kiehlmann and W. Schmidt, "An Analysis of the New Pion Form Factor Data ", Karlsruhe Preprint (March 1975).

[8]C. F. Cho and J. J. Sakurai, "A Simple Estimate for the Charge Radius of the Pion", Lettere al Nuovo Cimento 2, 7 (1971).

[9]G. Hohler and E. Pietarineh, "Electromagnetic Radii of Nucleon and Pion", Phys. Letters 53B, 471 (1975).

[10]G. Shaw, "Isovector Form Factors and the Rho-Prime", Phys. Letters 39B, 255 (1972).

[11]Frank S. Crawford, Jr., "Pion-Electron Scattering Cross Section at 1.12 BeV/c", Phys. Rev. 117, 1119 (1960).

[12]J. Allan et al., "Pion-Electron Scattering at 16 GeV/c", Nuovo Cimento 32, 1144 (1964).

[13]D. Cassel, Ph.D. thesis, Princeton U., 1965 (unpublished).

[14]P. Shepard, "Pion-Electron Scattering at Serpukhov", Bull. Am. Phys. Soc. 17, 435 (1972).

[15]G. T. Adylov et al., "The Pion Radius", Phys. Letters 51B 402 (1974).

[16]D. Drickey et al., "A Measurement of the Pion Form Factor by Direct Pion-Electron Scattering", Fermilab Proposal No. 216 (May 1973), Fermilab Library.

[17]D. Stork et al., "E216 Progress Report and Request for Running Time" (May 1975), Fermilab Library.

[18]C. May et al., "Proposal to Test Apparatus..." (May 21, 1975), Fermilab Library.

[19]See for example C. J. Bebek et al., Phys. Rev. D9, 1229 (1974).

[20]C. N. Brown, private communication.

[21]C. J. Bebek et al., "Electroproduction of K^+ Mesons in the Forward Direction", Phys. Rev. Lett. 32, 21 (1974).

[22]See for example M. M. Block et al., Phys. Rev. 169, 1074 (1968).

[23]C. Ankenbrandt et al., "Elastic Scattering of $\pi^\pm$, $K^\pm$, $p^\pm$ at Small Angles: A Preliminary Analysis", Fermilab-Conf. 75/61 - EXP (August 1975).

FIGURE CAPTIONS

Fig. 1: Diagrams illustrating (a) the direct determination of F_π or F_K, (b) determination of F_π by electroproduction, (c) possible determination of F_K by electroproduction, and (d) K* exchange, which interferes with (c).

Fig. 2: (a) The experimental layout for this form factor experiment, and (b) the original configuration for E69.

Fig. 3: Meson-electron elastic scattering kinematics: laboratory momenta and angles vs. Q^2.

Fig. 4: Geometrical acceptance vs. Q^2 for π-e and K-e at 200 GeV/c.

Fig. 5: Low-Q^2 π-e signal observed in experiment E69.

Fig. 6: The expected uncertainty in effective pole mass (or equivalently in radius) vs. running time for various assumed <u>a priori</u> uncertainties in absolute normalization.

Fig. 1

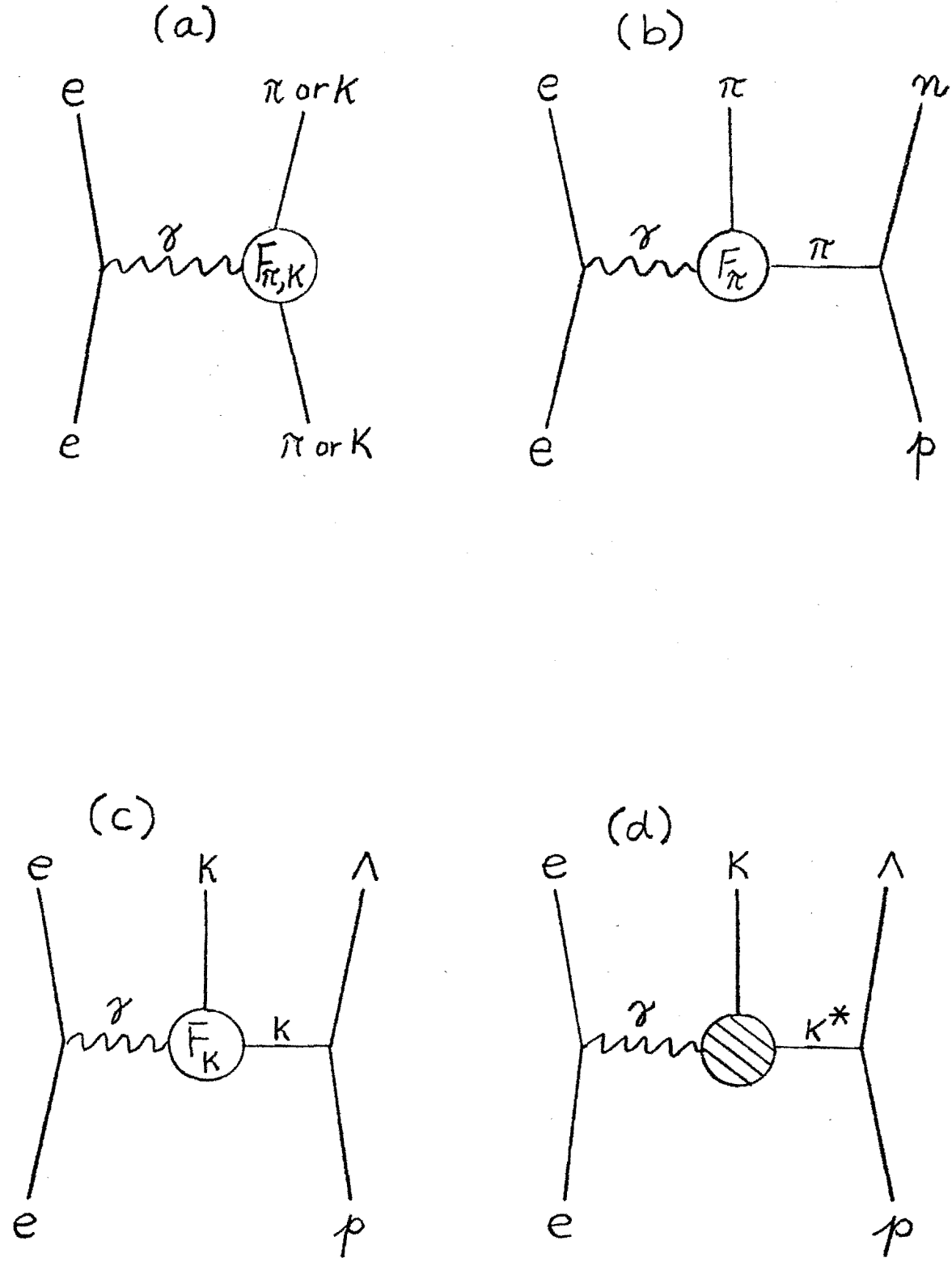

Fig. 2

(a) APPARATUS FOR MESON FORM FACTOR EXPERIMENT

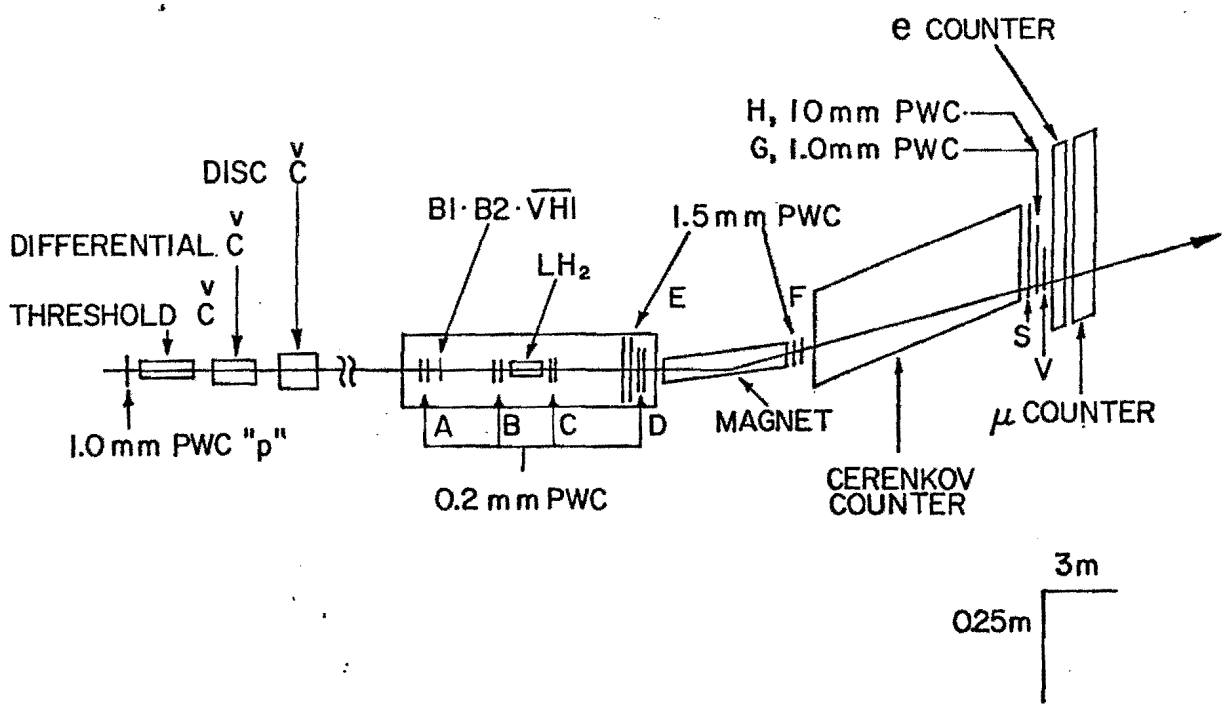

(b) E 69 APPARATUS

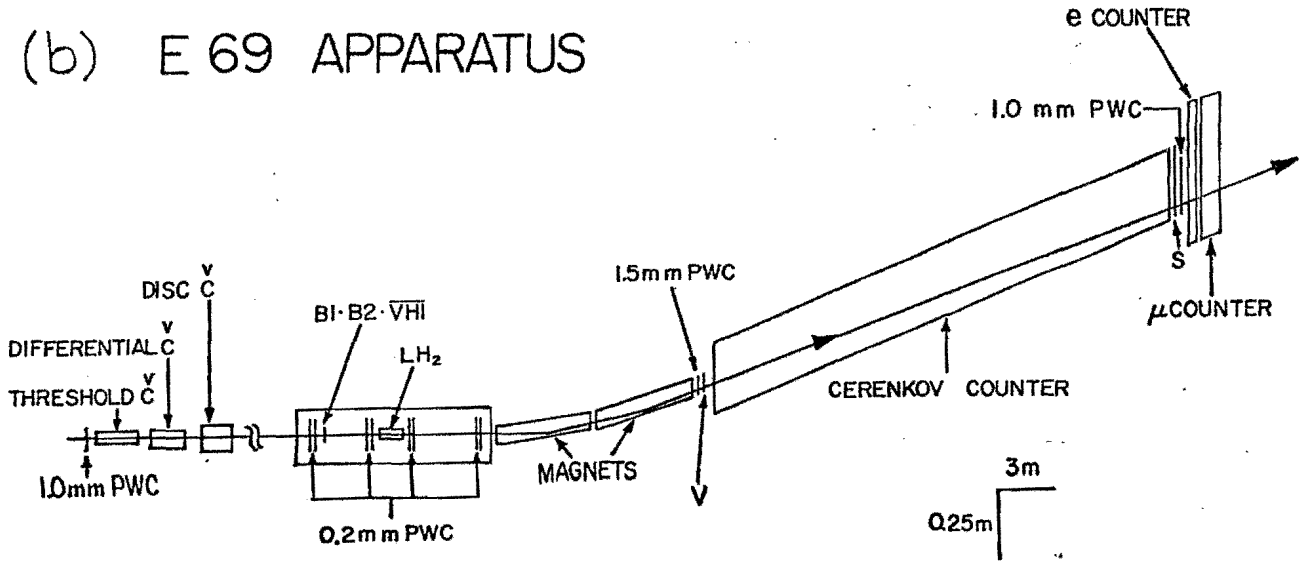

Fig. 3

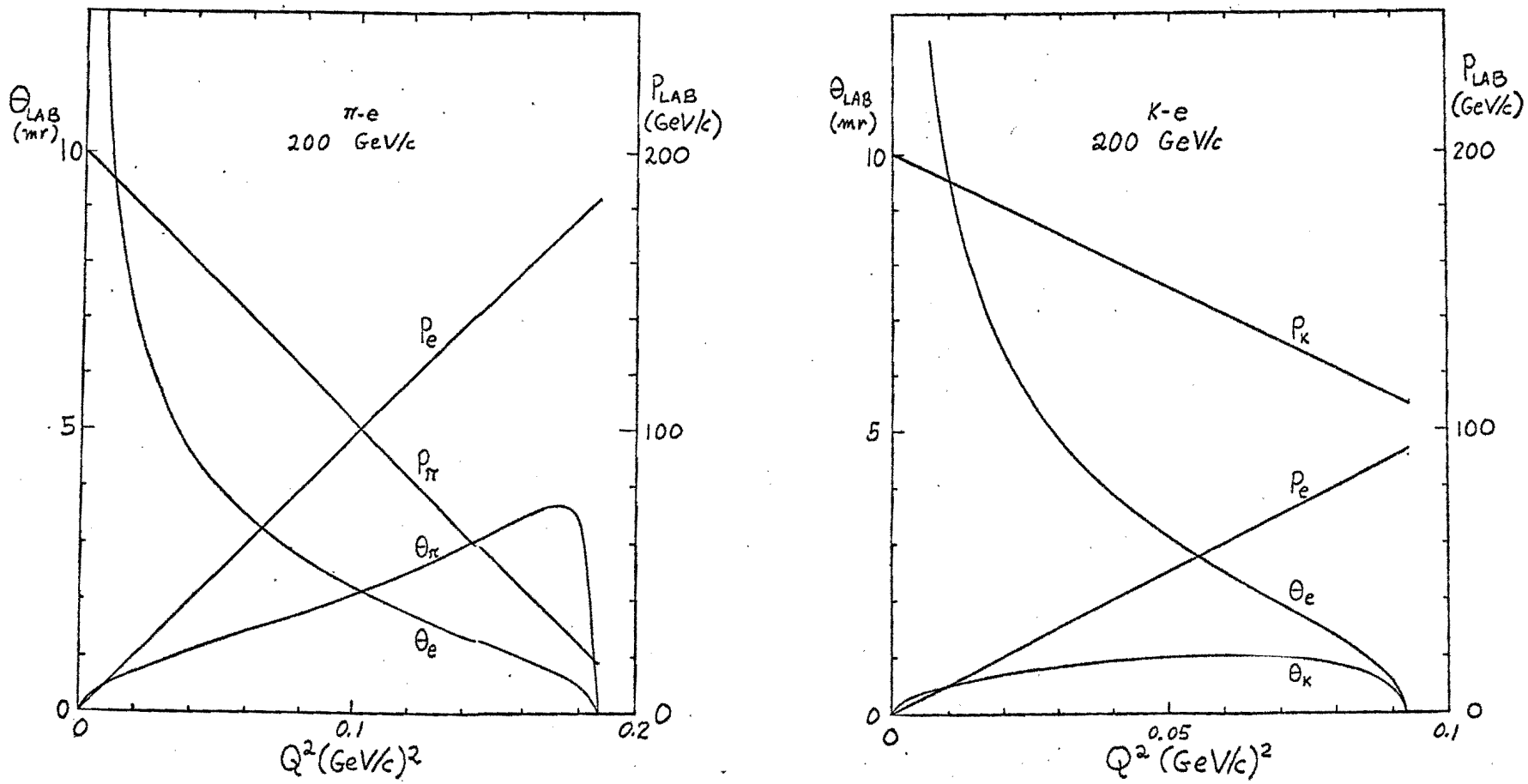
π-e
200 GeV/c
θ_{LAB} (mr)
P_{LAB} (GeV/c)
P_e
P_π
θ_π
θ_e
Q^2 (GeV/c)^2
K-e
200 GeV/c
P_K
P_e
θ_e
θ_K

Fig. 4

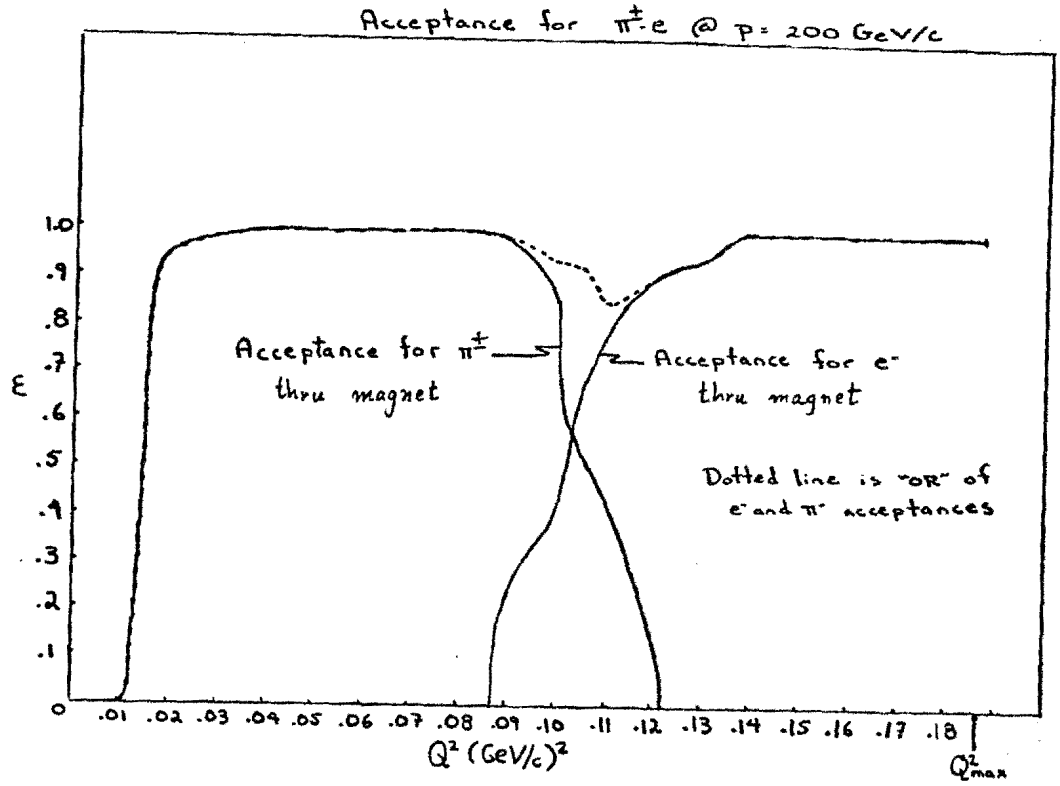
Acceptance for $\pi^{\pm}$-e @ p = 200 GeV/c
ε
1.0
.9
.8
.7
.6
.5
.4
.3
.2
.1
0
Acceptance for $\pi^{\pm}$ thru magnet
Acceptance for e⁻ thru magnet
Dotted line is "OR" of e⁻ and π⁻ acceptances
.01 .02 .03 .04 .05 .06 .07 .08 .09 .10 .11 .12 .13 .14 .15 .16 .17 .18
Q^2 (GeV/c)^2
Q^2_{max}

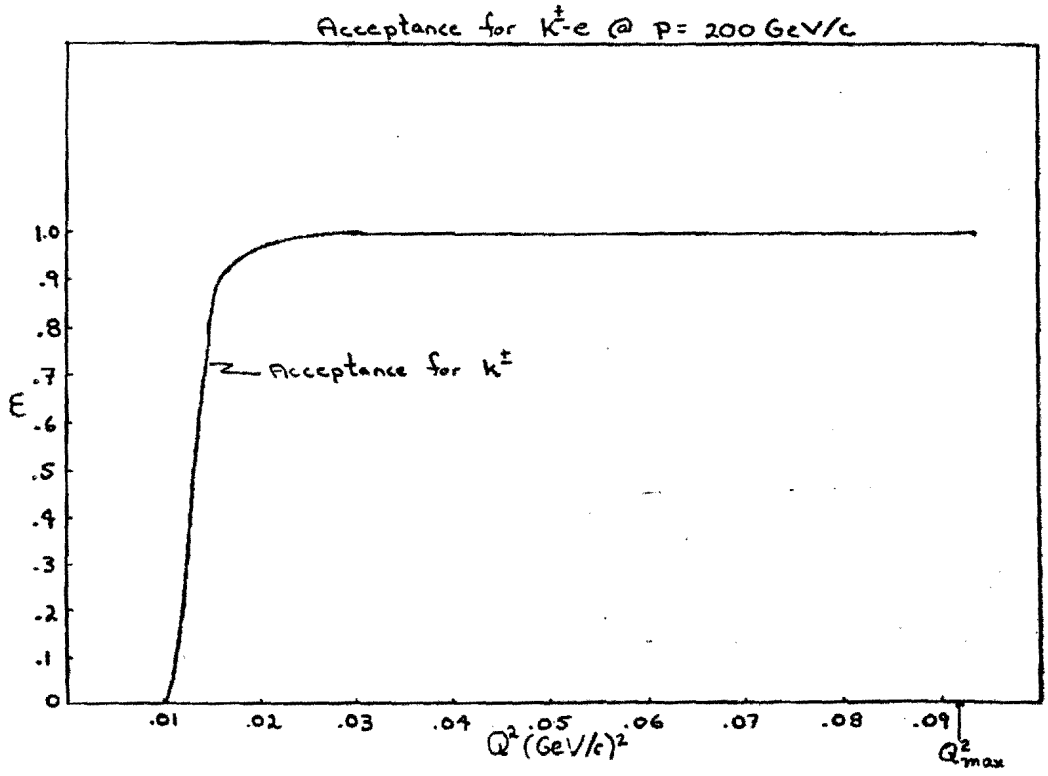
Acceptance for $K^{\pm}$-e @ p = 200 GeV/c
ε
1.0
.9
.8
.7
.6
.5
.4
.3
.2
.1
0
Acceptance for $K^{\pm}$
.01 .02 .03 .04 .05 .06 .07 .08 .09
Q^2 (GeV/c)^2
Q^2_{max}

Fig. 5. Recoil Mass^2 @ P = +150 GeV/c
π^+-e Scattering

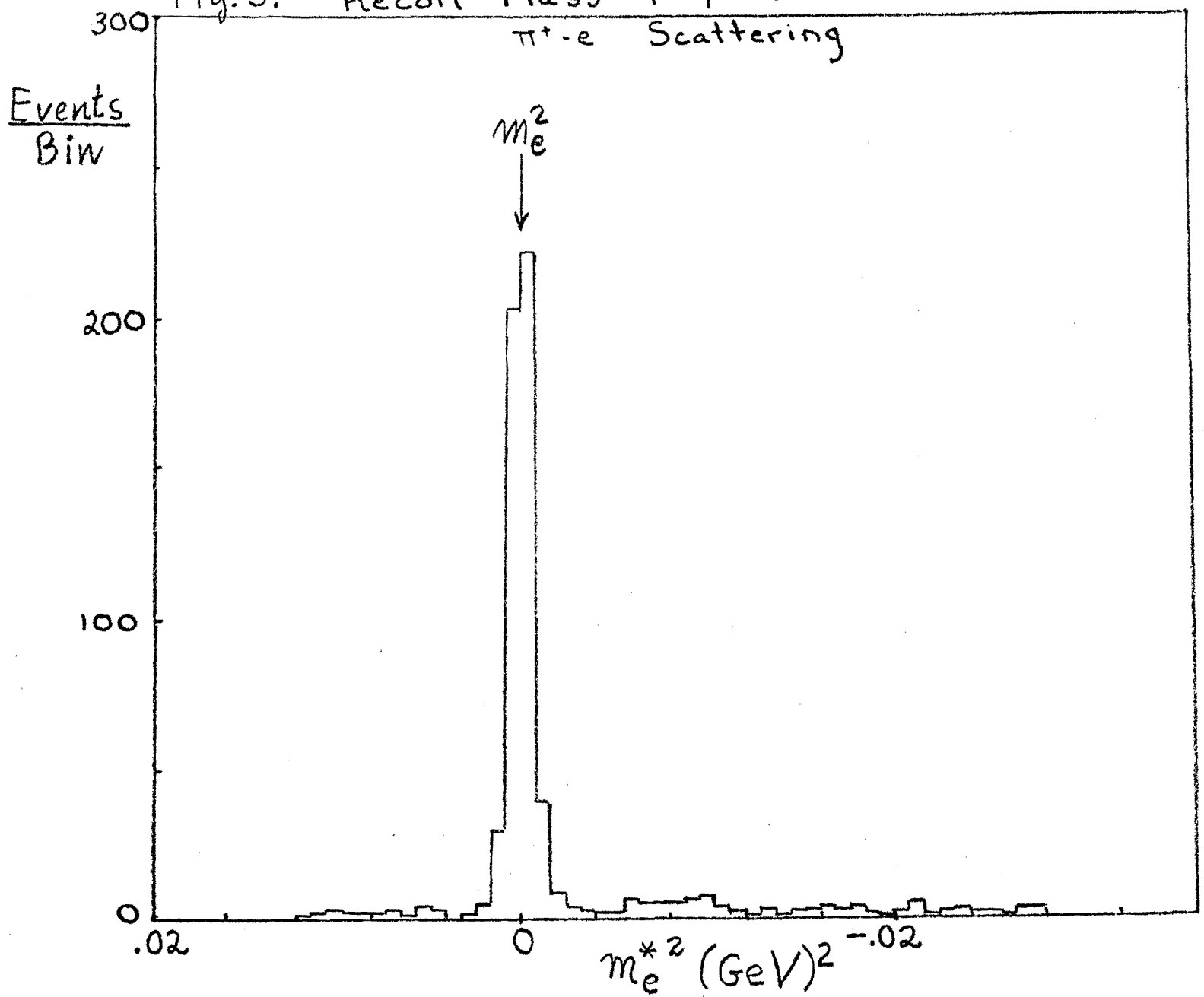

Fig. 6

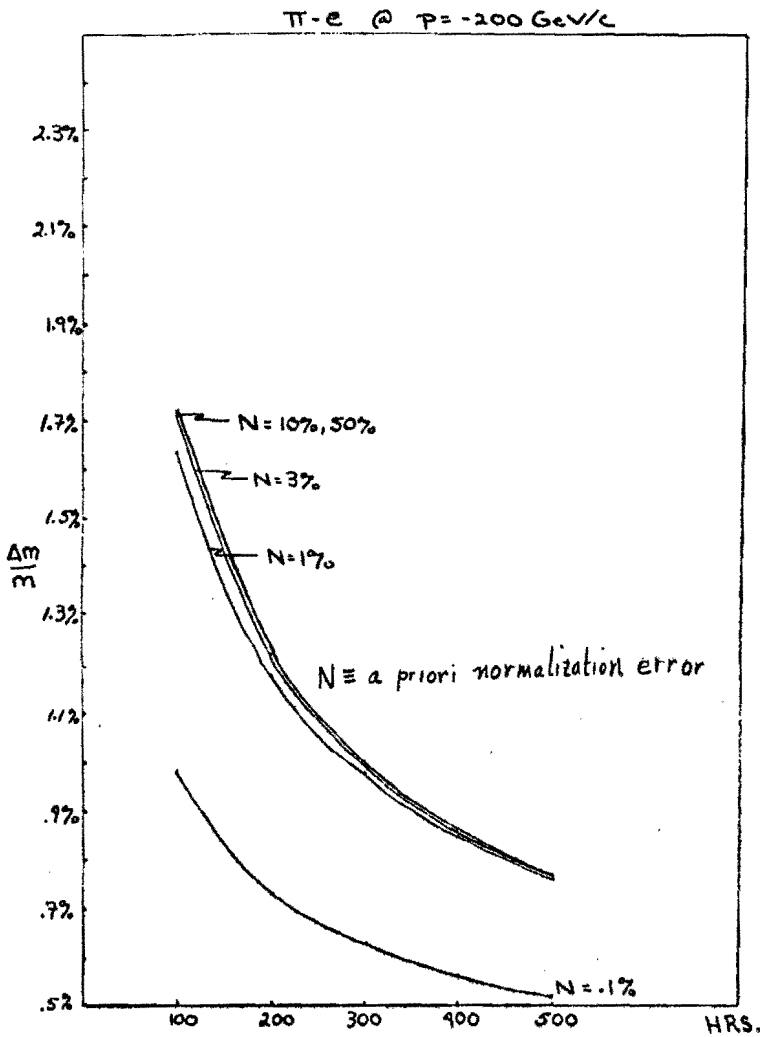
π-e @ p=-200 GeV/c
2.3%
2.1%
1.9%
1.7%
1.5%
1.3%
1.1%
.9%
.7%
.5%
Δm/m
N=10%, 50%
N=3%
N=1%
N ≡ a priori normalization error
N=.1%
100
200
300
400
500
HRS.

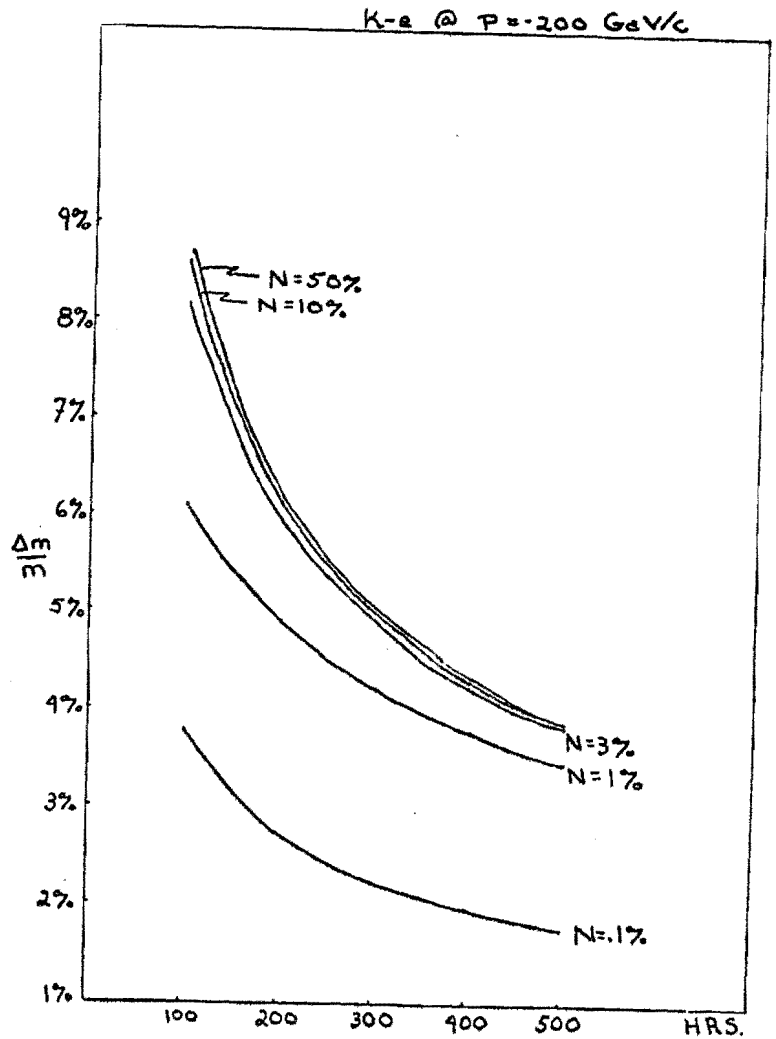
K-e @ p=-200 GeV/c
9%
8%
7%
6%
5%
4%
3%
2%
1%
Δm/m
N=50%
N=10%
N=3%
N=1%
N=.1%
100
200
300
400
500
HRS.

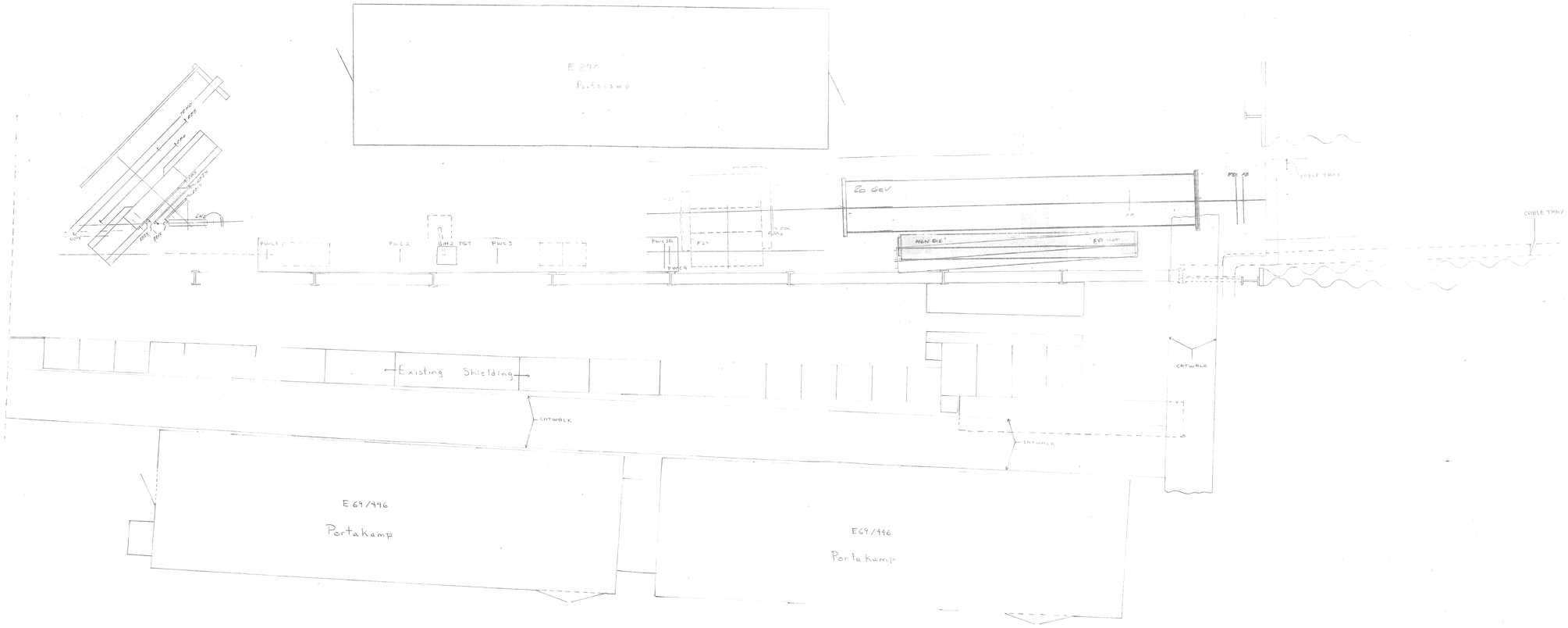

E 290
Portacamp
20 GeV
PWC1
PWC2
PWC3
PWC3A
PWC4
CABLE TRAY
CATWALK
Existing Shielding
E 69/446
Portakamp
E69/446
Portakamp